Physics

Electricity & Magnetism fields

Okayama University *Year* 2002

Analysis of the magnetic property of a permanent-magnet-type MRI - Behavior of residual magnetization

Norio Takahashi* Ryousuke Suenaga†
Koji Miyata‡ Ken Ohashi**

*Okayama University
†Okayama University
‡Shin-Etsu Chemical Corporation Limited
**Shin-Etsu Chemical Coporation Limited

This paper is posted at eScholarship@OUDIR : Okayama University Digital Information Repository.

http://escholarship.lib.okayama-u.ac.jp/electricity_and_magnetism/44

Analysis of the Magnetic Property of a Permanent-Magnet-Type MRI—Behavior of Residual Magnetization

Norio Takahashi, *Fellow, IEEE*, Ryousuke Suenaga, Koji Miyata, and Ken Ohashi

***Abstract*—The minor loops of B and H of steel due to pulse excitation and eddy currents induced in steel affect the magnetic characteristics of a permanent-magnet-type MRI. In this paper, the magnetic properties of a permanent magnet assembly is examined by using the finite-element method taking into account minor loop. The distribution of residual magnetization in the yoke is illustrated, and the effect of residual magnetization on the behavior of residual flux density is examined. It is shown that the behavior of B and H in minor loops is affected by the eddy currents in the yoke and pole piece.**

***Index Terms*—Finite-element method (FEM), minor loop, MRI.**

I. Introduction

A PERMANENT-MAGNET-TYPE MRI [1] for the whole body provides a viable alternative to a resistive and superconducting MRI. As the permanent magnet assembly contains pole pieces and yokes which are made of steel, minor loops of B and H due to pulse excitation and eddy currents induced in the steel affect the magnetic characteristics of the permanent magnet assembly. Although the behavior of B and H in minor loops due to the hysteresis of pole pieces has been investigated in a previous paper [2], the behavior of the residual flux density is different from measurement.

In this paper, the effects of minor loops and eddy currents in a yoke on the residual flux density are investigated. The detailed behavior of B and H in minor loops is illustrated using a simple model. It is shown that the minor loops and eddy currents in the yoke and pole piece affect the residual flux density considerably.

II. Analyzed Model

Fig. 1 shows the cross section of a permanent magnet assembly for an MRI device. The yoke is composed of two steel plates (square, 530 mm $\times$ 530 mm), two other steel plates (rings, ϕ 330 mm) each with a hole (ϕ 60 mm) and four columns. The permanent magnet (ring) has a hole (ϕ 60 mm). Although the actual assembly is three-dimensional (3-D) having four columns, it is simplified to an axisymmetric one when making FE calculations to reduce the CPU time and memory requirements. The yoke and pole piece are made of steel (SS400), and the conductivity is equal to 7.51×10^6 S/m. The magnetization of the Nd–Fe–B magnet is 1.21 T. The gradient coil having 15 turns is located on the surface of the pole piece.

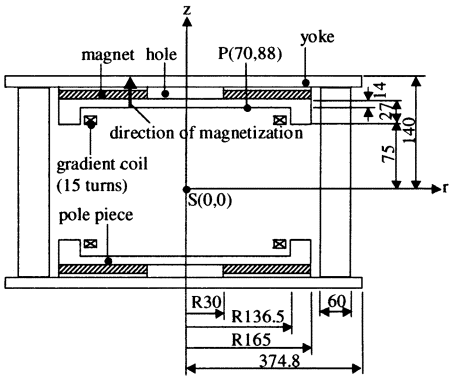

Fig. 1. Model of the permanent magnet assembly for an MRI device.

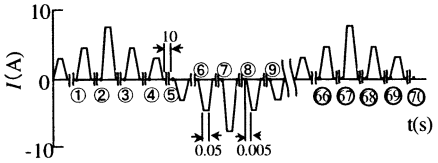

Fig. 2. Current of gradient coil.

Fig. 2 shows the current in the gradient coil as a function of time. The eddy currents flow in the yoke and pole piece due to the pulse excitation shown in Fig. 2. The eddy current distribution in the columns of the 3-D model and that of axisymmetric model are considerably different, and the amplitude of eddy current density in the axisymmetric model is much larger. Then, the eddy currents in the columns are neglected.

III. Method of Analysis

The eddy currents and nonlinear magnetic properties are taken into account in the analysis by using the step-by-step method. A relaxation factor [3] is introduced in the Newton–Raphson iteration technique in order to reduce the number of iterations. One quarter of the region is analyzed. The Neuman condition is imposed on the $z = 0$ boundary.

An upper part of the minor loop (loop2) is interpolated as shown in Fig. 3(a) using the measured hysteresis curves (loops 1 and 3) which are stored in a computer using the following relationship [2]:

$$\frac{P'P}{PP''} = \frac{P_1P_2}{P_2P_3} \tag{1}$$

Manuscript received June 18, 2002.

N. Takahashi and R. Suenaga are with the Department of Electrical and Electronic Engineering, Okayama University, Okayma 700-8530, Japan (e-mail: norio@eplab.elec.okayama-u.ac.jp; suenaga@eplab.elec.okayama-u.ac.jp).

K. Miyata and K. Ohashi are with Magnetic Materials R&D Center, Shin-Etsu Chemical Co. Ltd., Takefu 915-8515, Japan (e-mail: s03224@sec.shinetsu.co.jp; s05215@sec.shinetsu.co.jp).

Digital Object Identifier 10.1109/TMAG.2003.810510

0018-9464/03$17.00 © 2003 IEEE

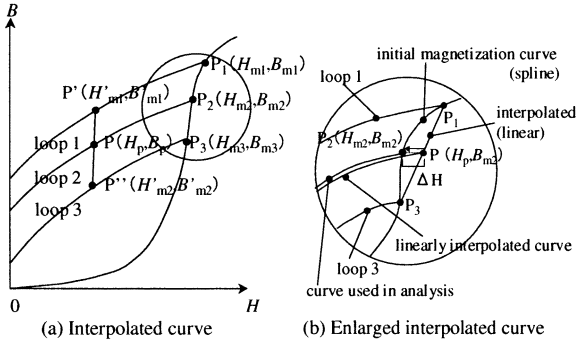

Fig. 3. Interpolation of curve.

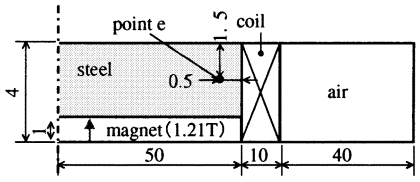

Fig. 4. Simple model (3-D axisymmetric model).

where, for example, $P'P$ denotes the length between two points P and P'. The initial magnetization and hysteresis curves are represented by a cubic polynomial. Some errors occur due to the linear interpolation as shown in Fig. 3(b). Then, the linearly interpolated curve is shifted horizontally by ΔH to avoid such an inconvenience as shown in Fig. 3(b).

A lower part of the minor loop is obtained from the upper part assuming that the lower part is symmetric with the upper one [2] like he Rayleigh loop. An error of such approximation is negligible when the amplitude of the minor loop is small [2].

IV. Behavior of B and H of a Simple Model

In order to check the appropriateness of the developed simulation software, the detailed behavior of B and H along the complicated minor loops is analyzed using a simple model shown in Fig. 4. One tenth of the amplitude of current (Fig. 2) in gradient coil is applied.

Fig. 5 shows the loci of B and H at a point e. The instants of ①, ②, ... in Fig. 5 correspond to ①, ②, ... in Fig. 2. B and H move along the minor loop in the direction of the arrow. At every pulse excitation, B and H move along the minor loop. When the current becomes zero after one pulse excitation, B and H become stable at points ①, ②, ... The operating range of B and H in Fig. 5(b) is wider than that in Fig. 5(a). This is caused by the skin effect due to eddy currents. This behavior suggests the appropriateness of the simulation of the minor loop.

V. Results and Discussion

Fig. 6 shows flux densities at instants ①, ②, ... at the point S in the gap (Fig. 1). They are periodically changed along with the current of the gradient coil for the case when hysteresis is taken into account only in the pole piece (case A), the case when hysteresis is taken into account in both pole piece and yoke (case B), the case when eddy currents in the yoke are also taken into account (case C), and the case when hysteresis and eddy currents

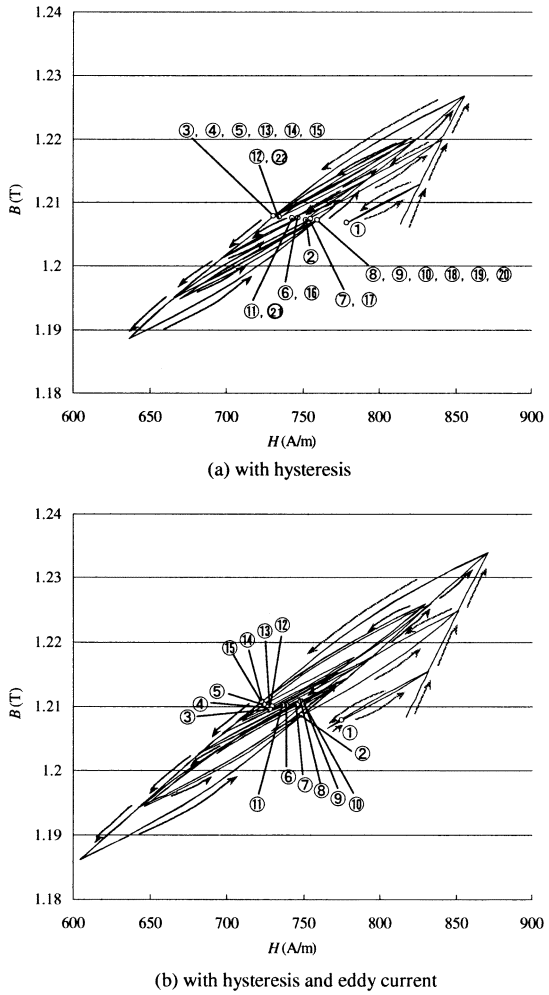

Fig. 5. Loci of B and H.

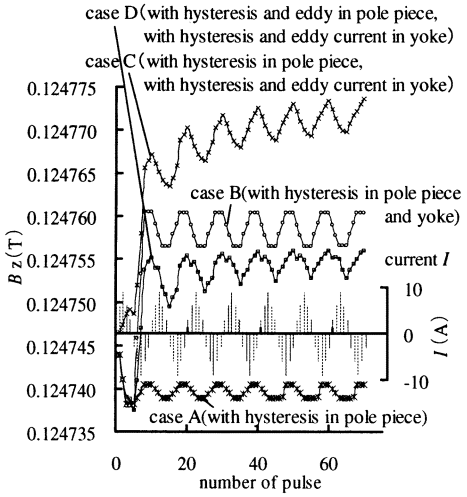

Fig. 6. Flux densities at instants ①, ②, etc. (point S in the gap).

in both the pole piece and yoke are taken into account (case D). The flux densities in Fig. 6 are the values at the instant when the transient phenomena are almost finished, but these values contain the result of the eddy current effect and hysteresis effect. The transient phenomena are shown later in Fig. 11.

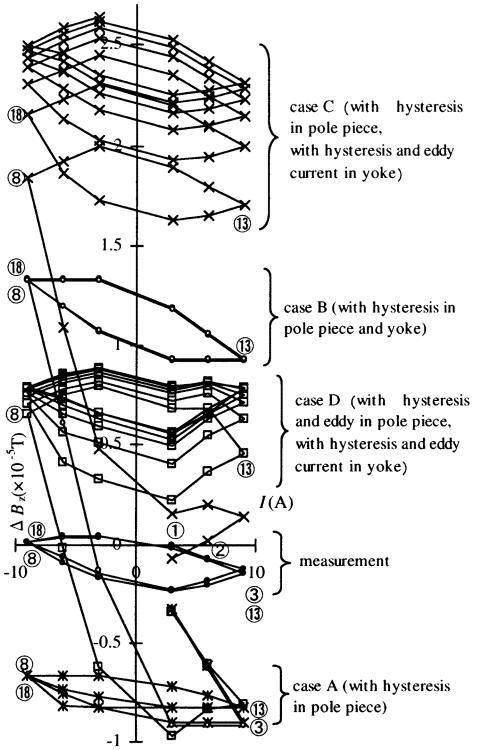

Fig. 7. Change of residual flux density ΔB_z (point S in the gap).

Fig. 7 shows the change of residual flux density ΔB_z at the point S in the gap, where a sensing coil is located. ΔB_z is given by

$$\Delta B_z = \Delta B_{zi} - B_{z0} \tag{2}$$

where B_{z0} is the flux density at the instant $t = 0$ ($I = 0$ A. B_{zi} is the flux density at the instant $t = i$ ($I = 0$ A). ⑧ and ⑱ are different from each other when eddy currents in the yoke is taken into account and those in the pole piece is neglected (case C). On the contrary, ⑧ and ⑱ have almost the same value in other cases A, B, and D. The behavior of ΔB in case D is not so different from the measured value in Fig. 7, but the amplitude is different, because the analysis is assumed to be axisymmetric.

In order to investigate the mechanism of producing the residual flux density at point S, the distribution of ΔB_z in the yoke and pole piece is investigated. Fig. 8(a)–(c) shows the equi-ΔB_z lines in the pole piece and yoke of cases B, C, and D, respectively. ΔB_z on the surface of the yoke is very large when there are eddy currents in the yoke, as shown in Fig. 8(b). ΔB_z on the surface of pole piece and yoke is very large when there are eddy currents in both the pole piece and yoke, as shown in Fig. 8(c). This is caused by the skin effect due to eddy currents. Fig. 9(a)–(c) shows the equi-ΔB_z lines in the air of cases B, C, and D, respectively.

Fig. 10 shows the loci of B and H at points P_1, P_2, and P_3 shown in Fig. 8(b) (case C). Operating points of B and H at the points P_1 and P_3 move as well as those in Fig. 5. The hysteresis loop approaches an initial magnetization curve at high flux density. Then, it is assumed that there is no minor loop when B is more than 1.58 T in the calculation, and only measured hysteresis loops less than 1.58 T are stored in a computer. Therefore, there are no minor loops at the point P_2, the flux density of which is larger than 1.58 T.

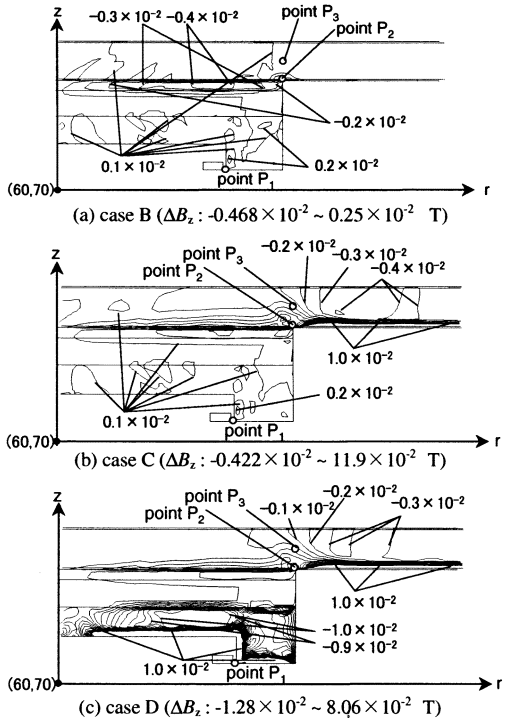

Fig. 8. Equi-ΔB_z lines in the pole piece and yoke (at the instant of ⑧).

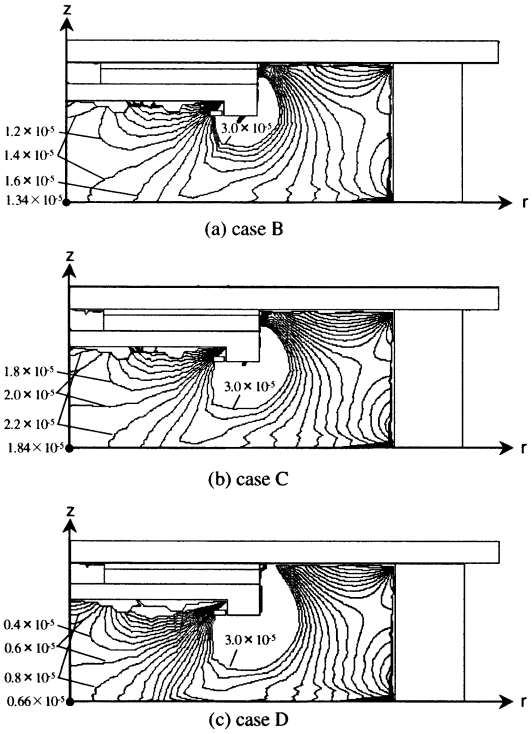

Fig. 9. Equi-ΔB_z lines in air (at the instant of ⑧).

Fig. 11 shows waveforms of B and I of cases B and C to investigate the effect of eddy current. The figure suggests that the flux density on the surface (point P_2) of the yoke is increased and the change of flux is delayed due to the skin effect.

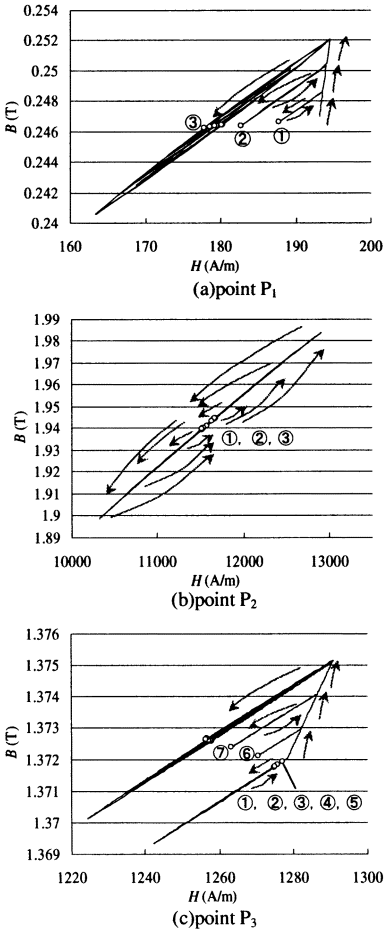

Fig. 10. Loci of B and H at various points (case C).

From Figs. 6–11, we can find the following.

1) When eddy currents flow in the yoke, the transient phenomenon remains long as shown in Fig. 6. Therefore, ΔB_z at the instant ⑧ and that at ⑱ are different.
2) When eddy currents flow in both the pole piece and yoke (case D), the transient phenomenon is not as prominent, as shown in Fig. 6, as the eddy currents flow mainly in the pole piece. ΔB_z of cases A, B, and D converge to the periodic one faster than that of case C.
3) The flux density on the surface of the yoke (point P_2) becomes large due to the skin effect as shown in Fig. 11(b)(ii), when eddy currents flow. Therefore, ΔB_z on the surface of the yoke is also increased as illustrated in Fig. 8(b). As a result, ΔB_z in the air (point S) becomes large (case C) as shown in Fig. 9(b). On the contrary, ΔB_z in the air (point S) is not so large in case B, because the flux density in the pole piece and yoke is not so concentrated when there is no eddy current. ΔB_z in the air (point S) in case D is also small, because there exist plus ΔB_z and minus ΔB_z (plus and minus values are nearly the same) in the pole piece due to the remarkable skin effect.

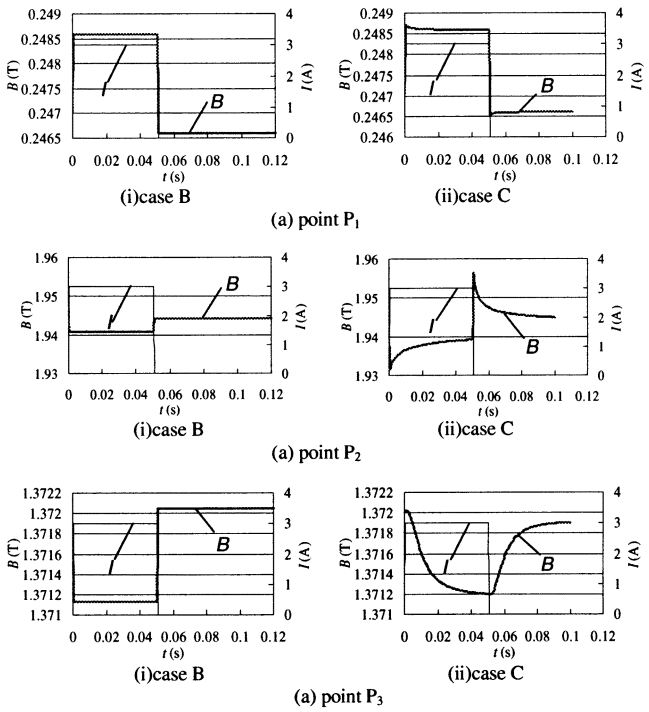

Fig. 11. Waveforms of B and I at various points.

VI. Conclusion

The results obtained are summarized as follows.

1) It is shown that the behavior of B and H along minor loops under pulse excitation is different in each position of the pole piece and yoke due to the skin effect.
2) The residual flux density ΔB_z becomes large when eddy currents flow in the yoke. This is because the flux density on the surface of the yoke is increased due to the skin effect, then the change of flux density becomes large.
3) It is illustrated that ΔB_z can be reduced when the flux density is not concentrated or the flux density in some region of the pole piece is higher and smaller than the average value due to the skin effect, resulting in plus and minus values of ΔB_z.

The detailed magnetic field analysis taking account of the minor loop and eddy current which was discussed in the paper will give a useful suggestion for improving the resolution of the MRI device.

References

[1] T. Miyamoto, H. Sakurai, H. Takabayashi, and M. Aoki, "A development of a permanent magnet assembly for MRI devices using Nd–Fe–B material," *IEEE Trans. Magn.*, vol. 25, pp. 3907–3909, Sept. 1989.
[2] N. Takahashi, T. Kayano, K. Miyata, and K. Ohashi, "Effect of minor loop on magnetic characteristics of permanent magnet type of MRI," *IEEE Trans. Magn.*, vol. 35, pp. 1893–1896, May 1999.
[3] K. Fujiwara, T. Nakata, T. Okamoto, and K. Muramatsu, "Method for determining relaxation factor for modified Newton–Raphson method," *IEEE Trans. Magn.*, vol. 29, pp. 1962–1965, Mar. 1993.